



Short communication

# Hyperspectral dark-field microscopy of gold nanodisks

Daniel Grasseschi, Filipe S. Lima, Marcelo Nakamura, Henrique E. Toma\*

Instituto de Química, Universidade de São Paulo, Zip Code 26077, CEP 05513-970, São Paulo, Brazil

## ARTICLE INFO

### Article history:

Received 10 September 2014  
 Received in revised form 31 October 2014  
 Accepted 31 October 2014  
 Available online 10 November 2014

### Keywords:

Gold nanodisks  
 Dark-field microscopy  
 Hyperspectral microscopy  
 Cytoviva microscopy  
 SPR

## ABSTRACT

The light scattering properties of hexagonal and triangular gold nanodisks were investigated by means of Cytoviva hyperspectral dark-field microscopy, exploring the huge enhancement of the scattered waves associated with the surface plasmon resonance (SPR) effect. Thanks to the high resolution capability of the dark-field microscope, the SPR effect turned it possible to probe the individual nanoparticles directly from their hyperspectral images, extrapolating the classical optical resolution limit, and providing their corresponding extinction spectra. Blue spectral shifts involving the in-plane dipolar modes were observed for the hexagonal gold nanodisks in relation to the triangular ones, allowing their spectroscopic differentiation in the dark-field images.

© 2014 Elsevier Ltd. All rights reserved.

## 1. Introduction

When metallic nanoparticles of sub-wavelength dimensions are submitted to an oscillating electromagnetic field, coherent oscillations of the conduction band electrons can be induced, reaching a maximum at an appropriate resonance frequency. This phenomena, which generates an enhanced light scattering and absorption pattern, is known as Surface Plasmon Resonance (SPR) (Link and El-Sayed, 2003; Maier, 2007; Sardar et al., 2009). The particles size, shape and composition, and the chemical environment can have a dramatic effect on the nanoparticles optical properties by changing the charge distribution on the metallic surface (Burda et al., 2005; Jain et al., 2006; Link and El-Sayed, 2000; Millstone et al., 2009; Pastoriza-Santos and Liz-Marzán, 2008).

Small spherical nanoparticles present an isotropic charge separation on the surface, generating a single dipolar mode, while large particles generate quadrupolar modes. Nanorods can exhibit two dipolar modes associated with the charge separation along the transversal and longitudinal axes, leading to two optical extinction bands located at frequencies depending on the particle dimensions and their aspect ratio. For flat nanoparticles, such as disks or triangles, two in-plane and two out-of-plane modes can be involved, from their corresponding dipoles and quadrupoles (Millstone et al., 2009; Pastoriza-Santos and Liz-Marzán, 2008).

Each mode leads to a different enhancement of the electromagnetic field, but the effect is particularly strong for particles exhibiting sharp tips, such as triangles and stars. Those particles show a great Surface Enhancement Raman Scattering (SERS) response due the high electric field concentration on the particle's tips (Hermoso et al., 2013). In order to explore the metallic nanoparticles as optical or SERS sensors (Stewart et al., 2008) it is important to understand the single particles properties. It should be noted, however, that nanoparticles fall typically below the limit of resolution of the conventional optical microscopes ( $\sim\lambda/2$ ).

Recent progress in dark-field microscopy has extended the optical resolution limit to  $\lambda/5$  due the higher resolution power from the oblique illumination employed, coupled with a cardoid annular condenser (Vodyanoy et al., 2007). The use of this technique is particularly rewarding in the case of plasmonic nanoparticles, because, in addition to a higher resolution, the enhanced light scattering propagates as a cone, generating a magnification response which allows the optical detection of the individual nanoparticles (Fan et al., 2012; Hu et al., 2008; Sherry et al., 2006). By means of the coupled spectral detector, it is possible to record the single nanoparticles scattering spectra, and to generate the corresponding hyperspectral images from the collected data.

In this work we report the optical properties of hexagonal and triangular gold nanodisks of thickness and diameters in the range of 1–15 and 20–60 nm, respectively, based on hyperspectral dark-field microscopy. The scattering spectra of the individual nanoparticles are presented and discussed in terms of the resonance effect involving distinct dipole and quadrupole modes.

\* Corresponding author at: Instituto de Química, Universidade de São Paulo, São Paulo, SP, Brazil. Tel.: +55 11 3091 3887.

E-mail address: [henetoma@iq.usp.br](mailto:henetoma@iq.usp.br) (H.E. Toma).

## 2. Materials and methods

### 2.1. Gold nanoparticles synthesis

Gold nanodisks (AuND) were synthesized with the following procedure: aliquots of  $\text{HAuCl}_4$   $10 \text{ mmol dm}^{-3}$  were added to 10 mL of dodecyltrimethylammonium triflate (DTATf)  $50 \text{ mmol dm}^{-3}$  aqueous solution ( $45^\circ\text{C}$ ) with gentle mixing, providing final concentrations of  $\text{HAuCl}_4$  varying from 0.25 to  $1 \text{ mmol dm}^{-3}$ . The solution was maintained at this temperature for 10 min, when  $60 \mu\text{L}$  of ascorbic acid (AA)  $100 \text{ mmol dm}^{-3}$  was added, changing gradually the starting yellow solution to a pink or purple color, depending on  $[\text{HAuCl}_4]$ .

### 2.2. Atomic force microscopy

The AFM samples were prepared by drop casting a gold nanoparticles suspension (diluted 100 times), on atomic flat mica (Ted Pella Inc.) and dried under vacuum. The images were recorded on a PicoSPM I microscope attached to a Molecular Imaging Picoscan 2100 controller. The topographic images were acquired by Intermittent Contact AFM technique, and using NCL-20 silicon cantilevers (Nanosensors).

### 2.3. Scanning electron microscopy (SEM)

After removing the excess of surfactant by centrifugation at 14,000 rpm for 3 min, the gold nanoparticles suspension was deposited on HOPG (highly ordered pyrolytic graphite), and dried under vacuum. The images were obtained using a JEOL model 7200 field emission electron microscope.

### 2.4. Electronic spectra

UV–vis absorption spectra were recorded on a Hewlett Packard 8453A diode-ray spectrophotometer, in the 190 to 1100 nm range, using a quartz cuvette.

### 2.5. Dark-field hyperspectral microscopy

A CytoViva ultra-resolution imaging system, composed by a dark-field hyperspectral arrangement mounted on an Olympus BX51 microscope, was used for recording the single particles Rayleigh scattering spectra. The dark-field configuration generates a hollow light cone focused on the specimen. Only the light scattered and diffracted inside the cone reaches the objective, which has a numerical aperture smaller than the numerical aperture of the dark-field condenser. The zero order diffracted light is not collected, and the particles appears as bright spots on a dark background. The resolution power is limited by the light diffraction. The CytoViva system uses an annular cardoid condenser (Vainrub et al., 2006) with high annular aperture that enables the collection of higher order diffracted light by the objective, increasing the resolution power up to  $\lambda/5$ . Fig. 1 shows an illustration of the experimental arrangement. Allied to the intensified light scattering by the plasmonic nanoparticles, this ultra-resolution optical system enables the study of a variety of nanoparticles, in wet media.

With this configuration it is possible to record a dark-field optical image composed by a three channel RGB spectra with a spatial resolution of 64 nm, and a hyperspectral image where each pixel has 64 nm and carries a full visible spectral information. For a better spectral signal to noise ratio a binning process can be performed, where four pixels are summed and a new pixel of 128 nm with an average spectra is generated. However, due the enhanced light scattering of the plasmonic nanoparticles, the full resolution hyperspectral image can be used in this case.

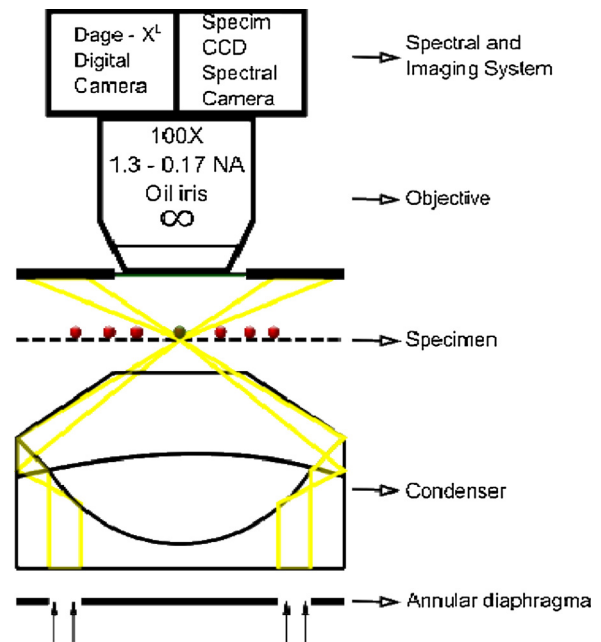


Fig. 1. Dark-field hyperspectral microscope scheme.

The sample was prepared by drop casting  $1 \mu\text{L}$  of Au nanoparticles suspension, after diluting by half with deionized water, on a NEXTERION® ultra-clean glass B (Schott). An ultra-clean NEXTERION® glass cover slip (Schott) was put over the drop, and sealed with adhesive tape to avoid oil penetration in the sample. The dark-field optical images and the Rayleigh scattering spectra were recorded with the sample wet, in order to keep the same refraction index.

## 3. Theoretical background

### 3.1. Theory of light scattering by metallic nanoparticles

The German physicist Gustave Mie made the first theoretical treatment of the light extinction process by particles with dimensions smaller than the wavelength of the incident light (Mie, 1908). By solving the Maxwell equations for electromagnetic waves interacting with spheres, Mie derived the extinction (ext) and scattering (sca) cross section expressions shown (1) and (2), related to the multipole oscillations. The absorption (abs) cross section can be obtained by subtracting the scattering cross section from de extinction cross section (3).

$$\sigma_{\text{ext}} = \frac{2\pi}{|k|^2} \sum_{L=1}^{\infty} (2L+1) \text{Re}(a_L + b_L) \quad (1)$$

$$\sigma_{\text{sca}} = \frac{2\pi}{|k|^2} \sum_{L=1}^{\infty} (2L+1) (|a_L|^2 + |b_L|^2) \quad (2)$$

$$\sigma_{\text{abs}} = \sigma_{\text{ext}} - \sigma_{\text{sca}} \quad (3)$$

In (1) and (2)  $k$  is the wave vector,  $a_L$  and  $b_L$  are composed by the particles refraction index, the refraction index of the medium and the particle radius.  $L$  refers to the excitation order, which is equal 1 for dipole excitations and 2 for quadrupoles (Fig. 2).

For nanoparticles with dimensions much smaller than the light wavelength ( $2r \ll \lambda$  or  $2r < \lambda/10$ ) only the dipolar oscillations contribute significantly for the extinction cross section (Link and El-Sayed, 2000) Thus, Eq. (1) can be simplified as shown in (4),

$$\sigma_{\text{ext}}(\omega) = 9 \frac{\omega}{c} \varepsilon_m^{\frac{3}{2}} V \frac{\varepsilon_2(\omega)}{[\varepsilon_1(\omega) + 2\varepsilon_m]^2 + \varepsilon_2(\omega)^2} \quad (4)$$

Download English Version:

<https://daneshyari.com/en/article/1588940>

Download Persian Version:

<https://daneshyari.com/article/1588940>

[Daneshyari.com](https://daneshyari.com)